Supporting Information

Hydrogen Incorporation in $Ru_xTi_{1-x}O_2$ Mixed Oxides Promotes Total Oxidation of Propane

Wei Wang,[1,2] Yu Wang,[1,2] Phillip Timmer,[2] Alexander Spriewald-Luciano,[2] Tim Weber,[2] Lorena Glatthaar,[2] Yun Guo,[1] Bernd M. Smarsly,[2]* Herbert Over[2]**

1) Key Laboratory for Advanced Materials, Research Institute of Industrial Catalysis, School of Chemistry and Molecular Engineering, East China University of Science and Technology, Shanghai 200237, China
2) Institute of Physical Chemistry, Justus Liebig University, Heinrich-Buff-Ring 17, D-35392 Giessen, Germany

* Correspondence: Herbert.Over@phys.chemie.uni-giessen.de; Bernd.Smarsly@phys.Chemie.uni-giessen.de; yunguo@ecust.edu.cn

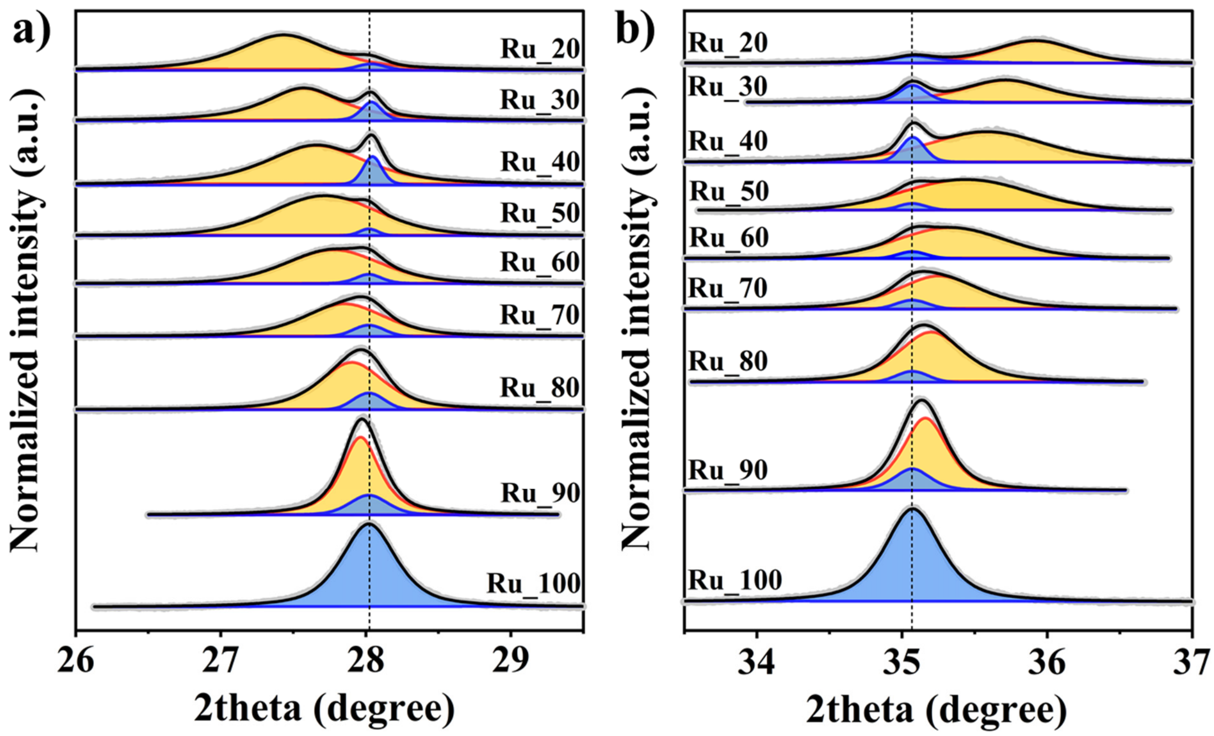

Figure S1: Decomposition of the (110) (a) and the (101) (b) reflection of Ru_x as a function of composition *x* in order to extract lattice parameters of the mixed phase.

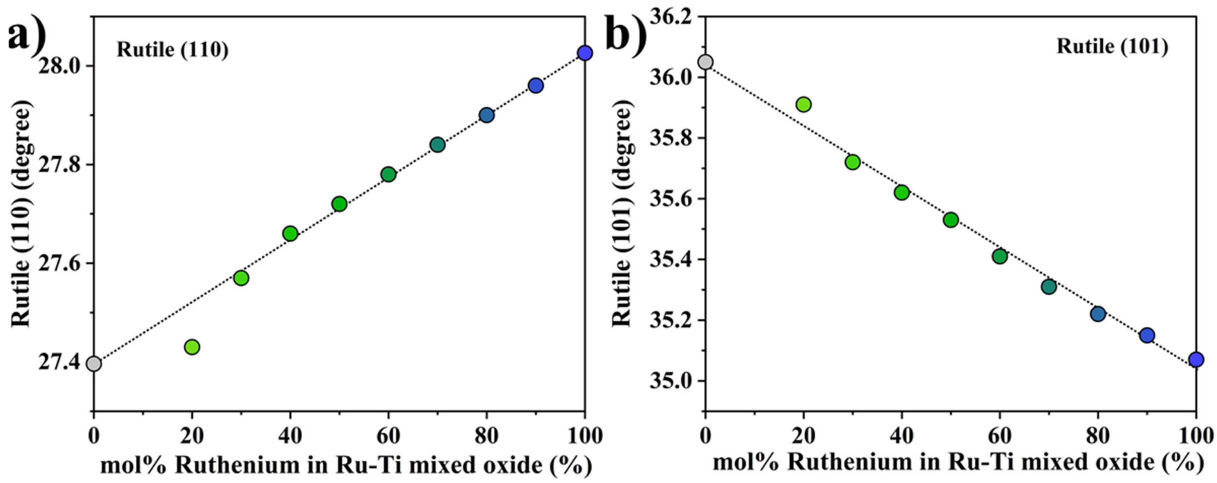

Figure S2: Peak shift of rutile (a) (110) and (b) (101) reflections in the mixed $Ru_xTi_{1-x}O_2$ oxide phase as a function of the nominal composition *x*.

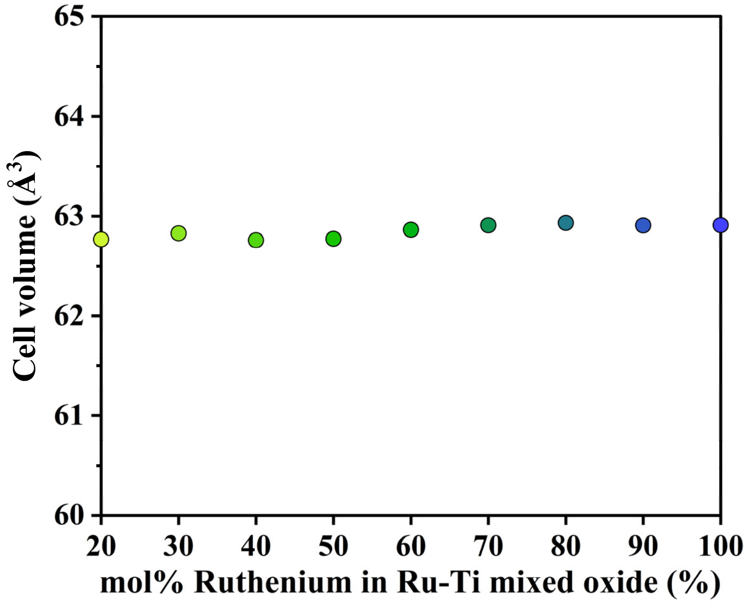

Figure S3: Calculated cell volumes of Ru_x as a function of composition *x* based on the unit cell parameters *a/b* and *c* of the mixed oxide $Ru_xTi_{1-x}O_2$ phase.

Table S1: Calculation of grain size and microstrain of Ru-Ti mixed oxides catalysts by Williamson-Hall method.

Catalysts	Grain size (RuO_2) (nm)[a]	Microstrain (RuO_2)[a]	Grain size (Ru-Ti) (nm)[b]	Microstrain (Ru-Ti)[b]
Ru_100	25.87	0.0020	-	-
Ru_90	29.17	0.0020	50.78	0.0020
Ru_80	36.08	0.0020	19.87	0.0004
Ru_70	54.85	0.0020	14.14	0.0006
Ru_60	72.16	0.0020	9.79	0.0008
Ru_50	137.11	0.0006	7.21	0.0002
Ru_40	114.26	0.0020	9.79	0.0040
Ru_30	72.16	0.0005	12.46	0.0020
Ru_20	69.15	0.0004	11.56	0.0002

a: Determined by Williamson-Hall method from the (110), (101), (020) and (111) reflections of RuO_2 phase.
b: Determined by Williamson-Hall method from the of (110), (101), (020) and (111) reflections of Ru-Ti mixed oxide phase.

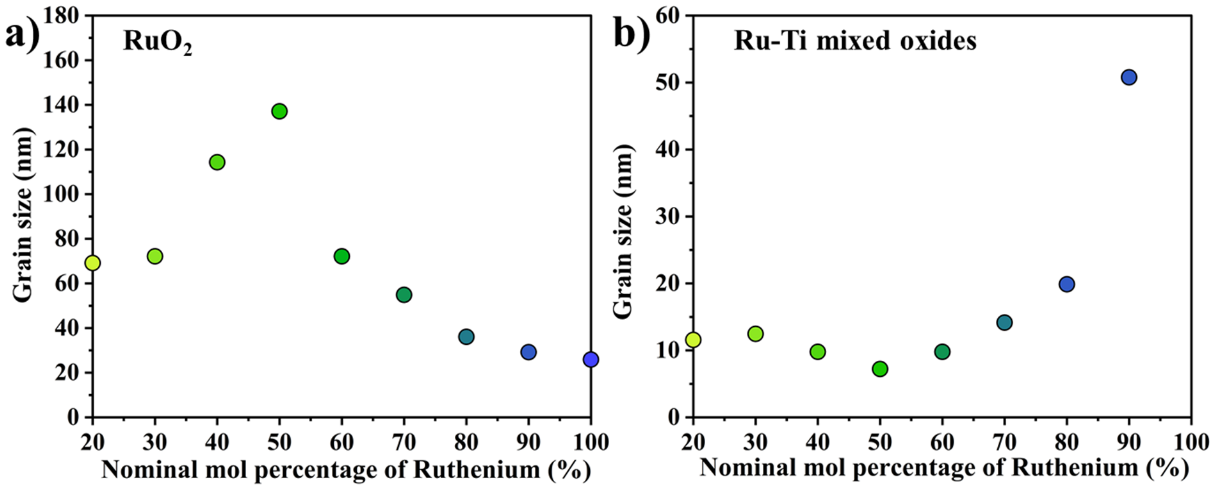

Figure S4: Calculated crystallite size of (a) RuO_2 phase and (b) Ru-Ti solid solution phase as a function of the nominal composition x given in mol% as determined by Williamson-Hall method.

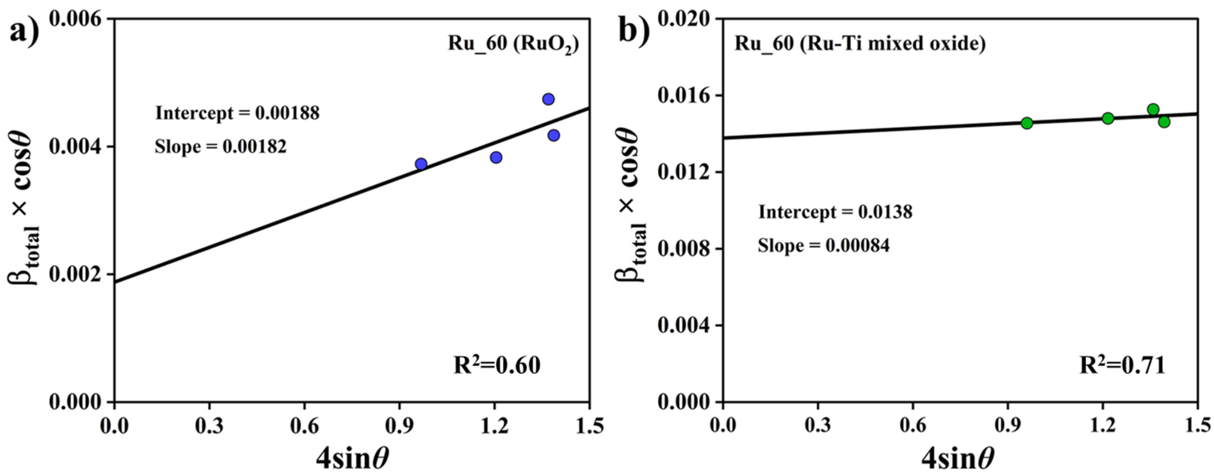

Figure S5: Williamson-Hall plot of (a) RuO_2 phase and (b) Ru-Ti solid solution phase as exemplified by Ru_60 sample.

Table S2: Optimized fitting parameters for the deconvolution of Ru 3d, Ru 3p, Ti 2p and O 1s photoelectron spectra used in our study.

	Ru3d-5/2		Ru3d-5/2 sat		Ru3d-3/2		Ru3d-3/2 sat		Ru3d-5/2 metal		Ru3d-3/2 metal	
Line shape	LF (0.4, 1, 45, 280)		LF (0.4, 1, 45, 280)		LF (0.6, 1, 45, 280)		LF (0.6, 1, 45, 280)		LF (1.2, 1, 400; 280)		LF (1.01, 1.25, 500, 50)	
Cat.	BE (eV)	FWHM	BE (eV)	FWHM	BE (eV)	BE (eV)	FWHM	BE (eV)	FWHM	BE (eV)	BE (eV)	FWHM
Ru_100	280.72	0.71	282.69	1.81	284.89	1.32	286.86	2.43	-	-	-	-
Ru_90	280.74	0.70	282.62	1.81	284.91	1.39	286.79	2.53	-	-	-	-
Ru_80	280.77	0.71	282.56	2.08	284.93	1.24	286.73	2.51	-	-	-	-
Ru_70	280.69	0.72	282.50	2.07	284.86	1.43	286.67	2.33	-	-	-	-
Ru_60	280.72	0.78	282.46	2.03	284.89	1.36	286.63	2.48	-	-	-	-
Ru_50	280.69	0.76	282.42	2.12	284.86	1.31	286.59	2.49	-	-	-	-
Ru_40	280.84	0.79	282.38	1.88	285.01	1.29	286.64	2.29	-	-	-	-
Ru_30	280.84	0.82	282.34	1.89	285.00	1.30	286.51	2.26	-	-	-	-
Ru_20	280.90	0.93	282.31	1.86	285.12	1.47	286.48	2.30	-	-	-	-
Ru_60_250R	280.83	0.85	281.59	1.89	285.00	1.22	285.75	2.10	280.25	0.58	284.42	0.95
Ru_60_250R_300O	280.80	0.74	282.43	2.05	284.97	1.29	286.60	2.1	280.28	0.68	284.45	0.95

	Ru3p-3/2		Ru3p-3/2 sat		Ru3p-1/2		Ru3p-1/2 sat		Ti2p-3/2		Ti2p-3/2	
Line shape	LF(1, 1, 45, 280)		LF(1, 1, 45, 280)		LF(1, 1, 45, 280)		LF(1, 1, 45, 280)		GL(30)		GL(30)	
Cat.	BE (eV)	FWHM	BE (eV)	FWHM	BE (eV)	FWHM	BE (eV)	FWHM	BE (eV)	FWHM	BE (eV)	FWHM
Ru_100	462.51	3.11	465.26	4.34	484.91	3.2	487.60	5.07	-	-	-	-
Ru_90	462.32	2.88	465.15	4.0	484.72	3.10	487.50	4.30	458.32	1.65	464.02	2.0
Ru_80	462.36	3.11	464.99	3.64	484.76	3.30	487.39	3.80	458.35	1.56	464.05	2.25
Ru_70	462.21	3.00	464.86	4.10	484.61	3.26	487.26	4.30	458.26	1.62	463.96	2.20
Ru_60	462.19	2.85	464.75	3.90	484.59	3.33	487.15	4.42	458.27	1.61	463.97	2.16
Ru_50	462.20	3.10	464.70	4.00	484.60	3.24	487.10	4.20	458.25	1.52	463.95	2.22
Ru_40	462.20	2.97	464.60	3.61	484.61	3.23	487.06	4.00	458.59	1.53	464.29	2.31
Ru_30	462.18	3.00	464.46	3.81	484.58	3.20	487.00	4.08	458.53	1.45	464.23	2.23
Ru_20	462.19	3.08	464.41	3.90	484.69	3.50	486.81	4.08	458.33	1.37	464.03	2.20
Ru_60_250R	461.73	2.90	463.76	4.10	484.13	2.90	486.16	4.15	458.27	1.33	463.97	2.29
Ru_60_250R_300O	462.09	3.09	464.56	4.11	484.49	3.10	486.96	4.11	458.27	1.41	463.97	2.17

	O-1s		OH/Oxygenated carbon	
Line shape	LF(0.37,1.2,25,110)		GL(30)	
Cat.	BE (eV)	FWHM	BE (eV)	FWHM
Ru_100	529.21	1.01	531.98	2.90
Ru_90	529.28	1.0	531.84	2.40
Ru_80	529.34	1.02	531.90	1.40
Ru_70	529.26	1.05	531.55	1.30
Ru_60	529.28	1.06	531.83	1.28
Ru_50	529.25	1.03	531.91	1.17
Ru_40	529.56	1.06	531.99	1.04
Ru_30	529.54	1.04	531.91	0.80
Ru_20	529.39	0.98	531.87	0.96
Ru_60_250R	529.56	1.06	531.87	1.19
Ru_60_250R_300O	529.37	0.99	531.78	1.39

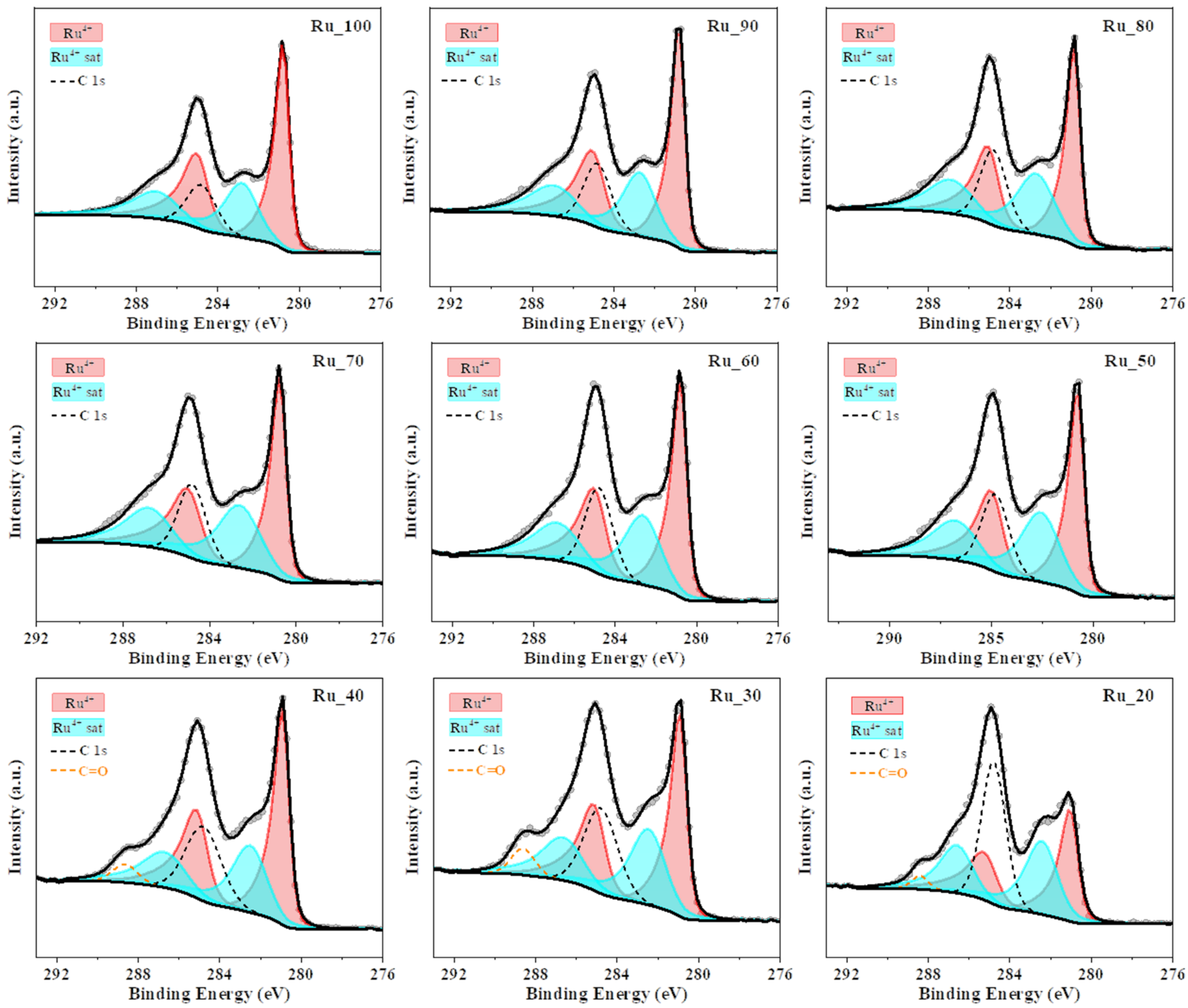

Figure S6: Deconvolution of Ru 3d XP spectra of freshly prepared Ru_x catalysts.

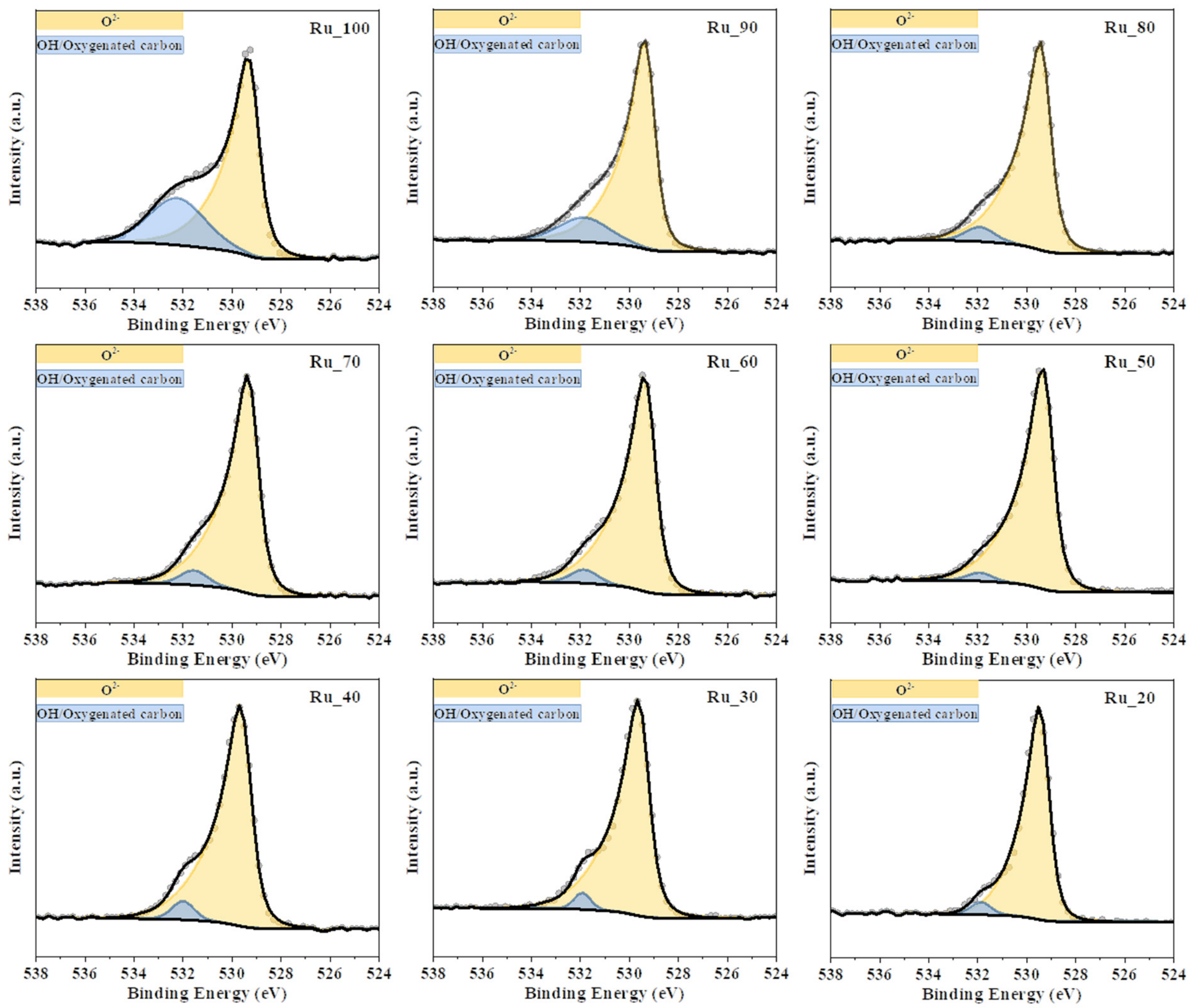

Figure S7: Deconvolution of O 1s spectra of freshly prepared Ru_x catalysts with varying composition *x*.

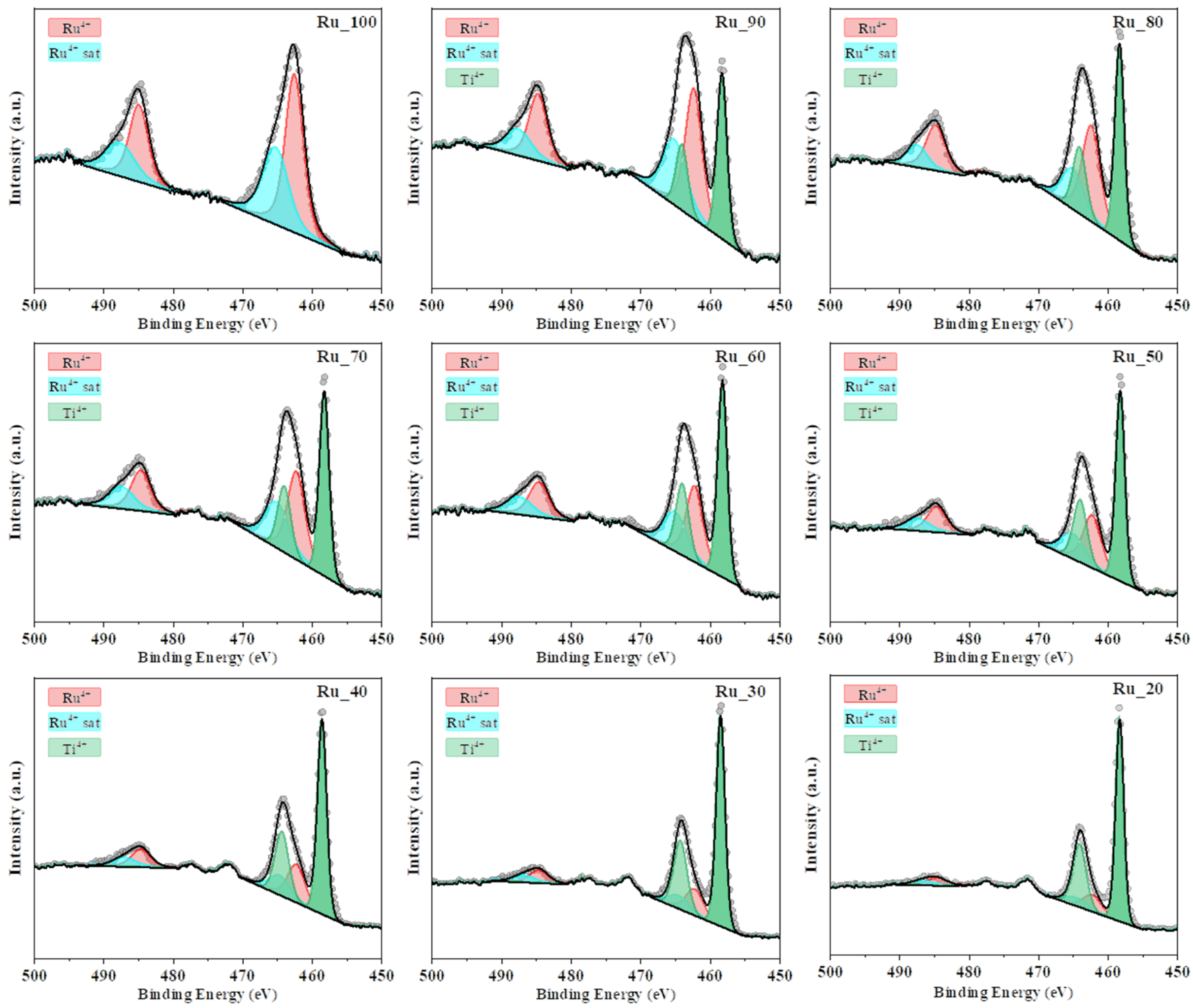

Figure S8: Deconvolution of Ru3p and Ti2p spectra of Ru_x catalysts with varying composition *x*.

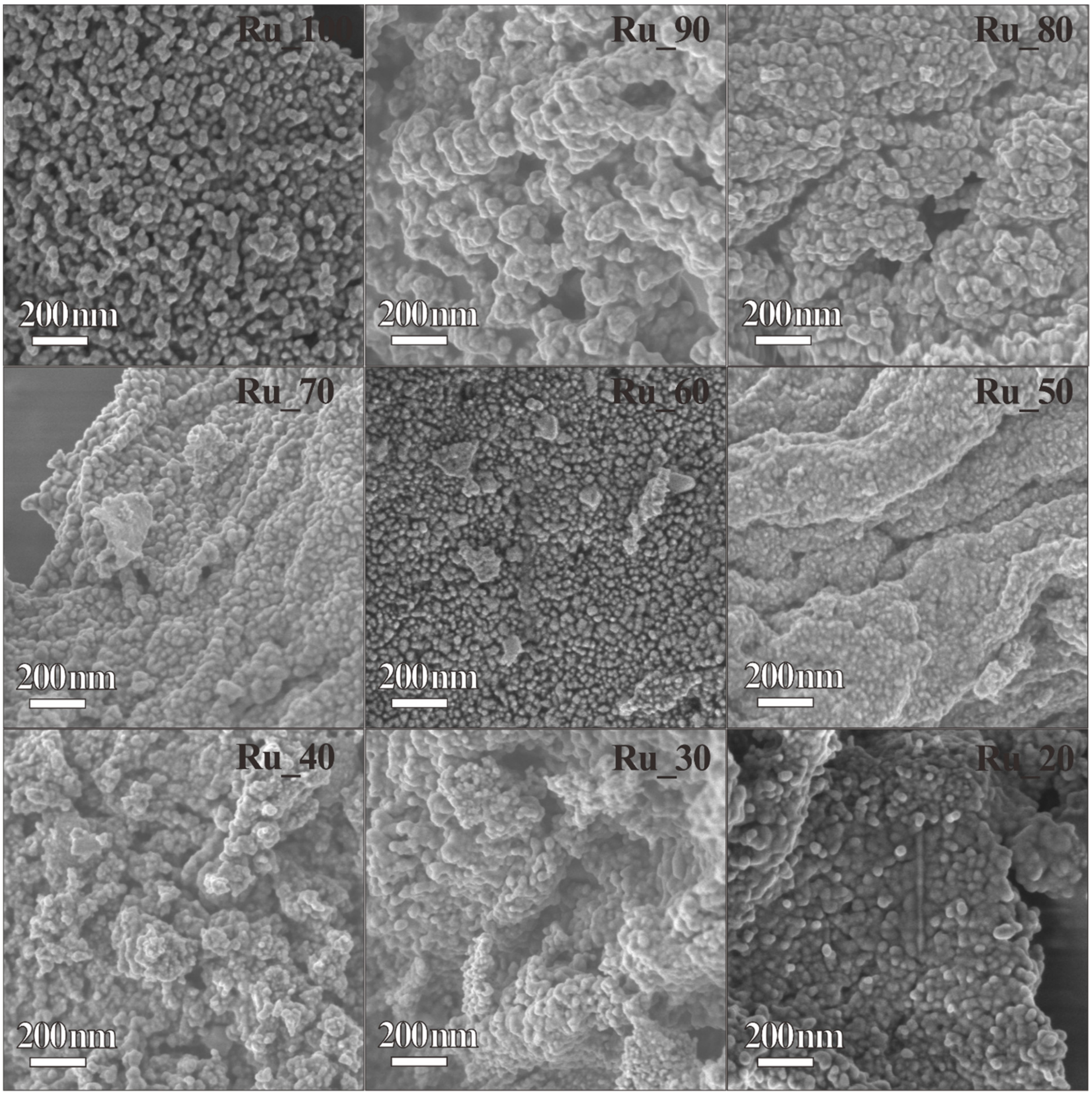

Figure S9: SEM micrographs for the various Ru_x samples.

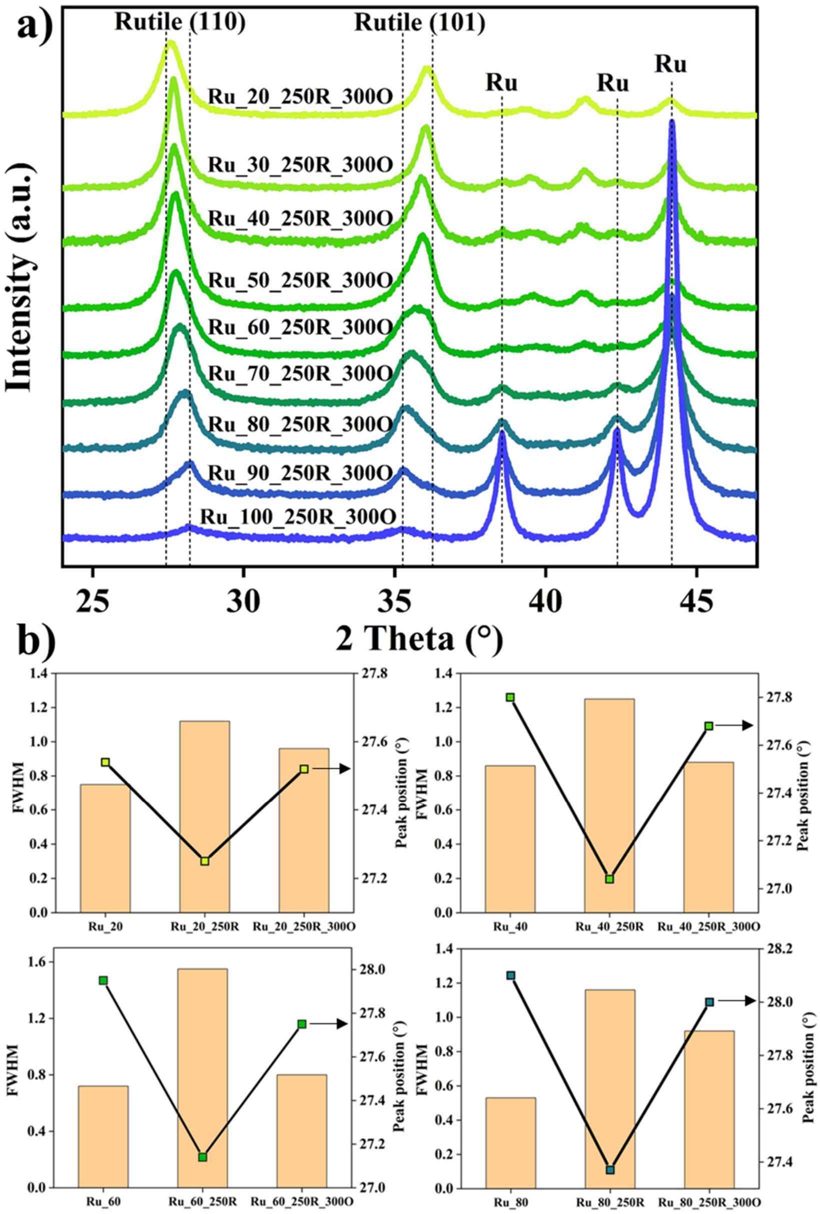

Figure S10: (a) XRD patterns of Ru_x_250R samples re-oxidized at 300 °C. (b) The changes of macrostrain (position) and microstrain (FWHM) of rutile (110) reflections of the Ru-Ti mixed oxide phase among the initial, reduced and re-oxidized Ru_x samples.

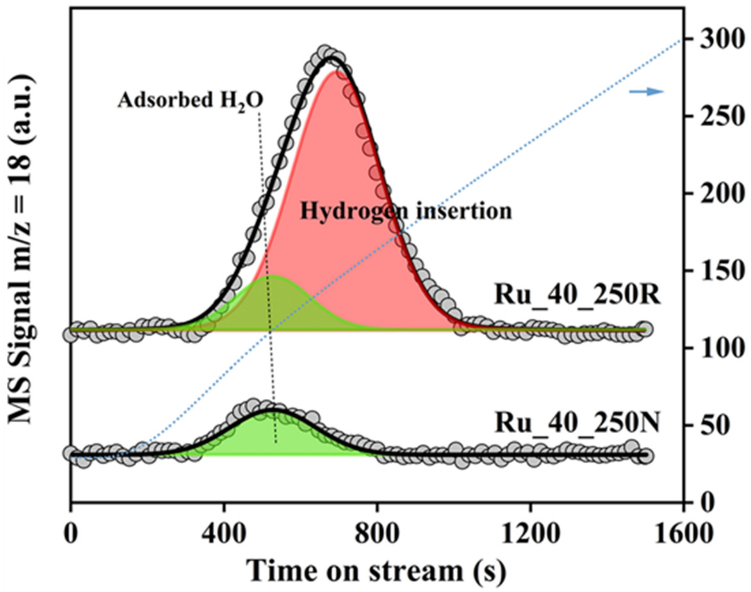

Figure S11: Peak deconvolution of H_2O signal (m/z = 18) of the Ru_40_250R and Ru_40_250N.

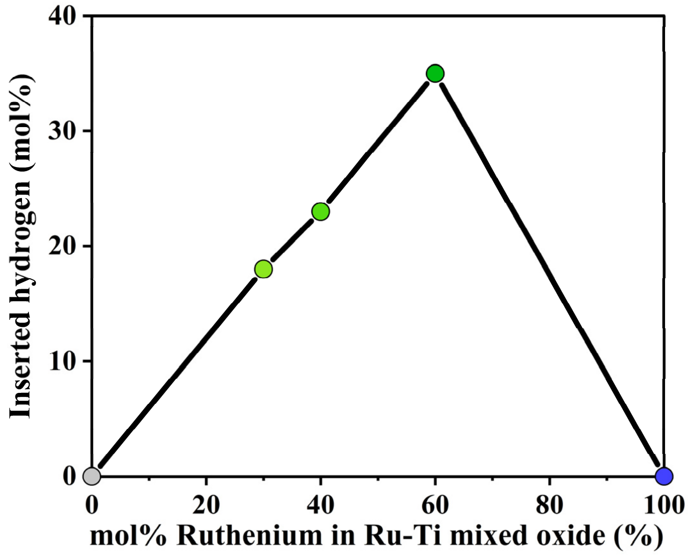

Figure S12: The calculated amount of incorporated hydrogen when varying the composition *x* of Ru_x.

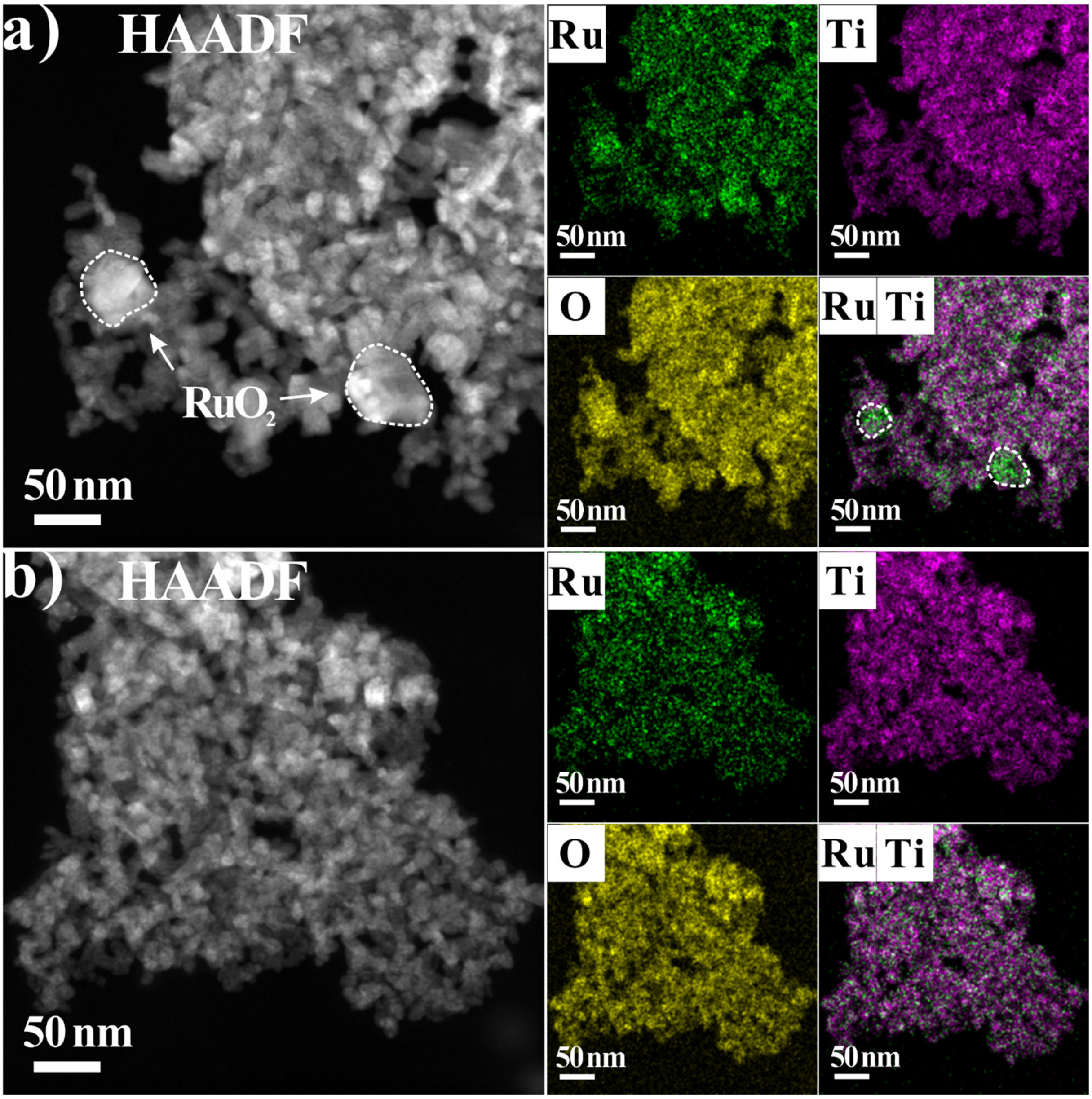

Figure S13: HAADF-STEM images and element mapping of (a) Ru_60 and (b) Ru_60_250R.

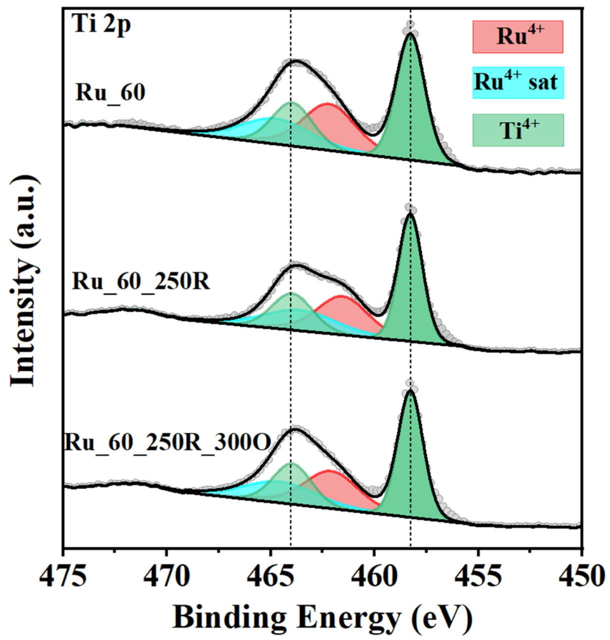

Figure S14: XPS-Ti 2p XP spectra of Ru_60, Ru_60_250R and Ru_60_250R_300O.

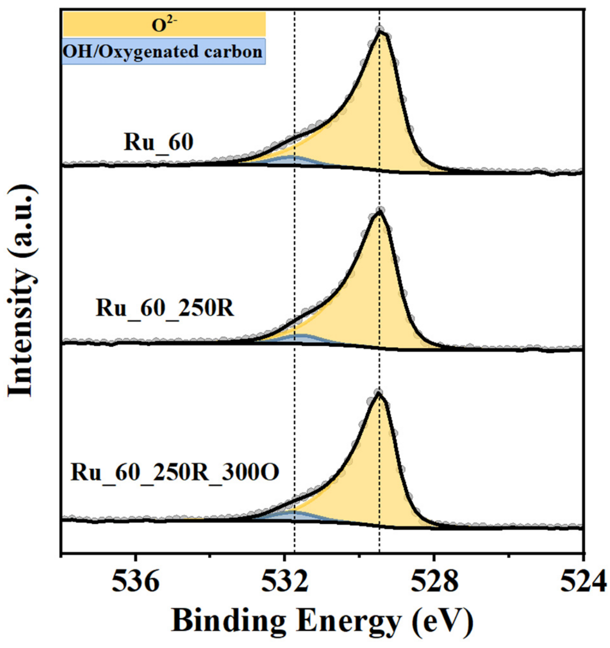

Figure S15: XPS-O 1s XP spectra of Ru_60, Ru_60_250R and Ru_60_250R_300O.

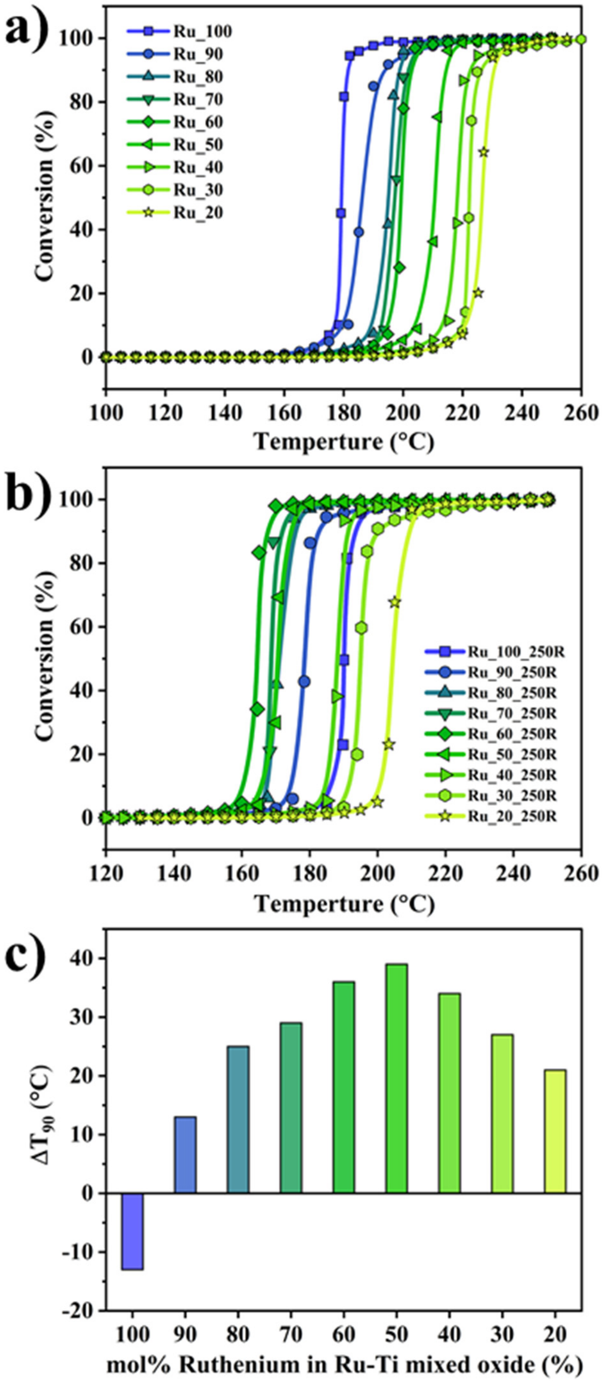

Figure S16: Light-off curves of catalytic propane combustion (1% propane, 5% O_2 balanced by 94% N_2) over Ru_x (b) and Ru_x_250R (b) (x ranging from 20% to 100% in steps of 10%) as a function of reaction temperature, when cycling the reaction temperature from 30 °C to 250 °C. The difference in T_{90}, i.e. the temperature, where 90 % conversion is reached, for Ru_x and Ru_x_250R is shown in panel c).

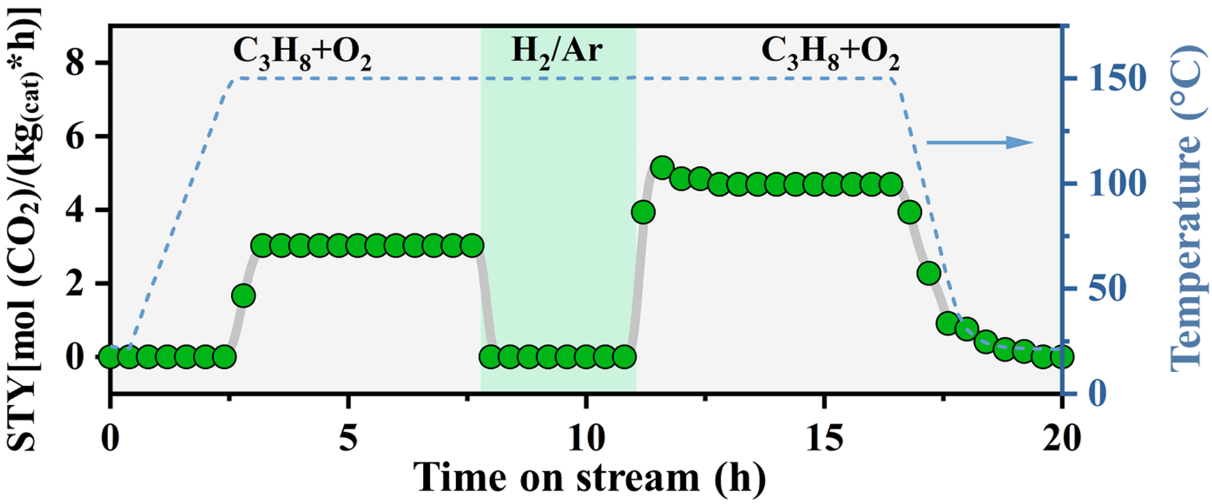

Figure S17. STY as a function of reaction time on catalytic propane oxidation over Ru_60_400R when keeping the reaction temperature at 150 ℃ (blue dotted line). The grey background represents total C_3H_8 oxidation conditions: 1 vol% C_3H_8, 5 vol% O_2, balanced by N_2; total volume flow: 100 sccm/min, temperature ramp: 1 K/min. The green background represents the gas mixture during heating and cooling stage: 4% H_2/Ar, total volume flow: 50 sccm/min. When reaching 150 ℃, the gas composition is switched to the reaction mixture (grey background).